Supporting Information

Exploring Ferrocene-Directed Photo-Fenton Initiation of RAFT Polymerization

Xiyang Zhang[1,#], Chaobin Pang[1,#], Xiaolu Wang[1], Shuyan Zhang[1], Lei Zhang[1,*], Wei Ji[1],Ling Huang[1], Yantong Li[2] and Su Jing[1,*]

School of Chemistry and Molecular Engineering, Nanjing Tech University, 30 South Puzhu Road, Nanjing 211816, Jiangsu, China

**Corresponding Author*

Contents

Experimental Section

Materials. Reagents and chemicals, including **Fc1** and S,S′-bis(α,α′-dimethyl-α″-acetic acid) trithiocarbonate (bis-TTC), were obtained from commercial sources and used without further purification, unless otherwise specified. *N,N*-Dimethylacrylamide monomer (DMA, 99%; Aladdin Industrial Corp., Shanghai, China) was passed through an aluminum oxide column prior to polymerization. Hydrogen peroxide (H_2O_2, 30 wt%) was used as received. Two ferrocenylseleno compounds, **Fc2** and **Fc3** (**Scheme S1**), were synthesized following previously reported procedures by our group[1-2].

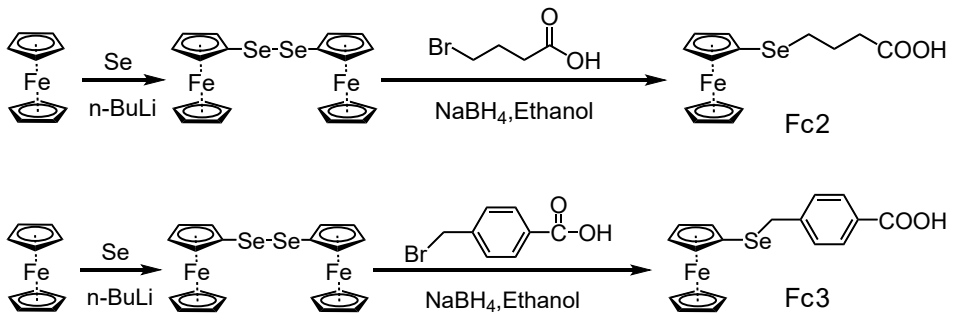

Scheme S1. Synthetic routs of **Fc2** and **Fc3**.

Characterization. Absorption spectra were measured using an ultraviolet–visible (UV–VIS) spectrometer (LAMBDA950; PerkinElmer, Rodgau, Germany). An AV400 spectrometer (Bruker, Billerica, MA, USA) was used to perform ^{1}H NMR spectroscopy. The molecular weight and polydispersity of PDMA were evaluated using gel permeation chromatography (GPC) conducted with a 1260 Infinity GPC analysis system (Agilent Technologies, Santa Clara, CA, USA) equipped with an Ultrahydrogel column (Waters, Milford, MA, USA). A 0.1 mol L^{-1} $NaNO_3$ solution was used as the eluent at a flow rate of 1 mL min^{-1}, and the analysis was performed at 40°C relative to polyethylene glycol (PEG) standards.

Molecular weight and end-group analysis of PDMA were performed using matrix-assisted laser desorption/ionization time-of-flight (MALDI-TOF) mass spectroscopy on an UltrafleXtreme mass spectrometer (Bruker) in linear positive mode. For MALDI-TOF mass measurements, the sample was dissolved in MeOH at a concentration of 10

mg·mL^{-1}. The matrix, trans-2-[3-(4-tert-butylphenyl)-2-methyl-2-propenylidene] malononitrile, was dissolved in THF at a concentration of 30 mg·mL^{-1}, and the cationization agent, sodium trifluoroacetate, was dissolved in acetone at a concentration of 19 mg·mL^{-1}. These three solutions were then mixed in a 1:1:0.1 volume ratio. Subsequently, 0.5 μL of the mixed solution was spotted onto a ground steel target plate, and the solvent was allowed to evaporate before analysis.

A 59.4 mg sample of polymers was dissolved in the digestion solution and diluted to a final volume of 50 mL before being analyzed using Inductively Coupled Plasma Optical Emission Spectroscopy (ICP-OES). Radio frequency power was 1150 W; flux of cooling air was 15 L·min^{-1}; flux of auxiliary air was 0.5 L·min^{-1}; flux of carrying-air was 0.55 L·min^{-1}; pump speed was 60 r·min^{-1}.

The radicals were identified by using an Electron Paramagnetic Resonance (EPR, Bruker A200-6/1) with DMPO as the spin-trapping agents. Typically, 45 μL of samples were mixed with 15 μL of 0.1 M DMPO aqueous solutions, after 5 minutes irradiation with 460 nm LED (100 mW·cm^{-2}) and then immediately transferred to EPR capillary tubes (0.5 mm, 100 mm) for measurement. The EPR was operated under the following conditions: microwave frequency 9.8 GHz, microwave power 2.0 mW, sweep time 30 s, modulation frequency 100 kHz and field center 3500 G.

The hydrodynamic diameter, zeta potential, and polydispersity of the nanoobjects were determined using a Zetasizer Nano ZS90 instrument (Malvern Instruments, Malvern, UK) at a fixed scattering angle of 90°. Transmission electron microscopy (TEM) images, energy-dispersive X-ray (EDX) spectroscopic analyses, and selected area electron diffraction (SAED) patterns were acquired using a Talos F200X G2 microscope operating at 200 kV. TEM samples were prepared by drop-casting onto a copper grid and dried at ambient temperature before measurement. For scanning electron microscope (SEM) measurements, a drop of solution was deposited onto a silicon wafer and dried at ambient temperature. Subsequently, the sample was coated

with gold and viewed using a Quanta 200 FEG electron microscope (FEI Ltd., Hillsboro, USA) operated at 10 kV. SEM images were recorded using a digital camera to observe the morphologies of the nanoobjects.

General Procedure for Fc-PF-RAFT Polymerization. The following components were mixed together in a 10 mL quartz tube open to the air: 1.0 mL of DMA (approximately 10 mmol), 1.0 mL of deionized water, 15 μL of 30 wt% H_2O_2, 14.2 mg of bis-TTC (0.05 mmol), and 0.6 mg of **Fc1** (0.0025 mmol). This resulted in a reaction system with a molar ratio of $[DMA]_0/[\mathbf{Fc1}]_0/[\text{bis-TTC}]_0/[H_2O_2]_0$ = 200:0.05:1:3. The reaction mixture was then mildly stirred under 460-nm light-emitting diode irradiation (100 $mW \cdot cm^{-2}$) for 15 min. Then, the **Fc1**-PDMA-**Fc1** sample was purified for further ^1H NMR and GPC characterizations. The **Fc**-PDMA-**Fc** (where **Fc** represents either **Fc2** or **Fc3**) polymers were synthesized using the same procedure as that for **Fc1**-PDMA-**Fc1**, with $[DMA]_0/[\mathbf{Fc}]_0/[\text{bis-TTC}]_0/[H_2O_2]_0$ ratios of 25:0.05:1:3, 50:0.05:1:3, or 100:0.05:1:3.

Fc1-PDMA-**Fc1**, ^1H NMR (400 MHz, DMSO-d_6) δ 5.03 (O*H*), 4.73–4.55 ([Fe(η^5-C_5H_5)(η^5-C_5H_4)]), 2.81 (–N(C*H*$_3$)$_2$), 1.13–1.52 (–C*H*$_2$–), 2.40 (–C*H*(CO)–CH$_2$–), 0.95 (–C(C*H*$_3$)$_2$COOH).

Fc2-PDMA-**Fc2**, ^1H NMR (400 MHz, DMSO-d_6) δ 5.02 (O*H*), 4.19–4.37 ([Fe(η^5-C_5H_5)(η^5-C_5H_4)]), 2.80 (–N(C*H*$_3$)$_2$), 1.13–1.57 (–C*H*$_2$–), 2.40 (–C*H*(CO)–CH$_2$–), 0.93 (–C(C*H*$_3$)$_2$COOH).

Fc3-PDMA-**Fc3**, ^1H NMR (400 MHz, DMSO-d_6) δ 7.07–7.92(–C_6H_4–), 5.03 (O*H*), 4.15–4.23 ([Fe(η^5-C_5H_5)(η^5-C_5H_4)]), 2.80 (–N(C*H*$_3$)$_2$), 1,12–1.57 (–C*H*$_2$–), 2.40 (–C*H*(CO)–CH$_2$–), 0.94 (–C(C*H*$_3$)$_2$COOH).

Evaluation of •OH Generation During Ferrocene-Directed Photo-Fenton Reaction. Methylene blue (MB) degradation experiments were conducted to investigate the •OH generation capability of **Fc1–Fc3** in the photo-Fenton reaction. In brief, a mixture containing 1 mL of MB (0.15 mM) in 0.1 M phosphate-buffered solution (pH = 5.7) was prepared and combined with 2 mL of 30 wt% H_2O_2 aqueous

solution (7.5 mM). The resulting solution was continuously stirred for 30 min prior to the addition of 0.025 mmol of **Fc1–Fc3**, with and without light irradiation. The •OH generation ability was subsequently evaluated by measuring the absorbance of MB at 665 nm using a UV–VIS spectrophotometer.

***In Situ* Chain Extension.** To demonstrate the high chain-end fidelity and livingness of synthetic polymers synthesized by Fc-PF-RAFT, polymers with DP values of 50 and 100 were selected for *in situ* chain extension experiments. The same amounts of all reagents used in the original reaction, including 1 mL of DMA, 1 mL of deionized water, 15 μL of 30% wt H_2O_2, and 0.0025 mmol of **Fc1**, were added to the reaction mixture for the chain extension step. After 15 min, the monomer conversion for both polymers had reached >90%, as confirmed by ^{1}H NMR analysis. Samples were diluted with deionized water for GPC analysis.

***In Situ* Self-Assembly After Fc-PF-RAFT Polymerization.** After Fc-PF-RAFT polymerization of DMA with bis-TTC and **Fc1–Fc3**, as described above, the systems were directly incubated at 4°C for 12 h. SEM and TEM samples were prepared for morphological characterization.

Supporting Data

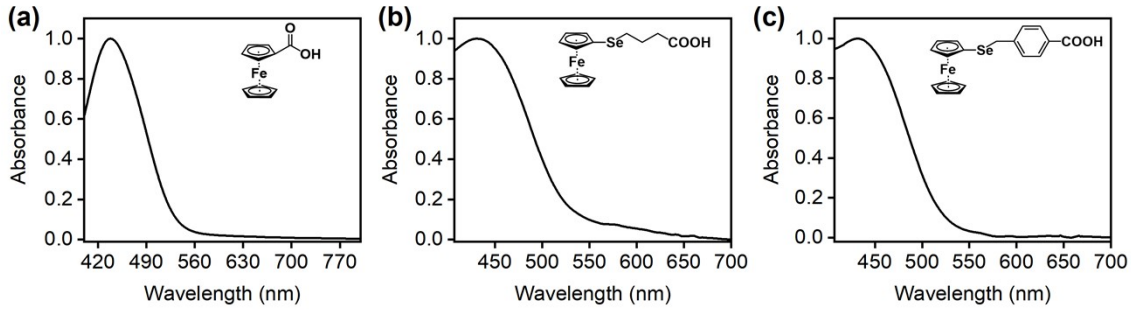

Figure S1. UV-Vis spectra of **Fc1**(**a**), **Fc2** (**b**) and **Fc3** (**c**).

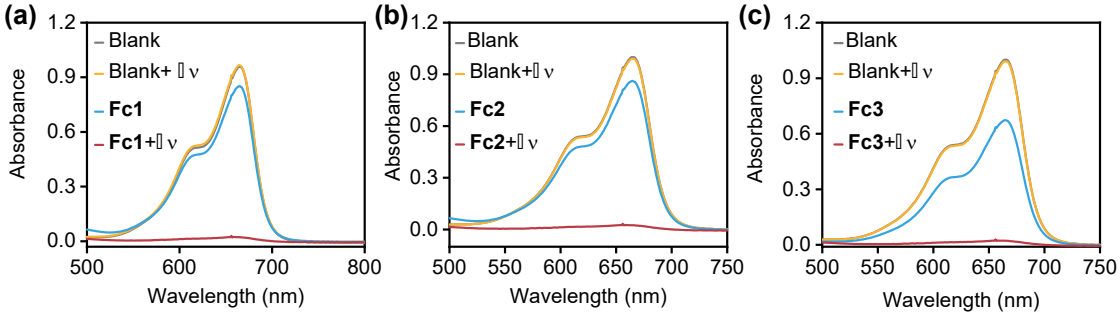

Figure S2. UV-Vis spectra of MB in the absence and presence of **Fc1** (**a**), **Fc2** (**b**) and **Fc3** (**c**)-based Fenton reaction before and after 460-nm light irradiation.

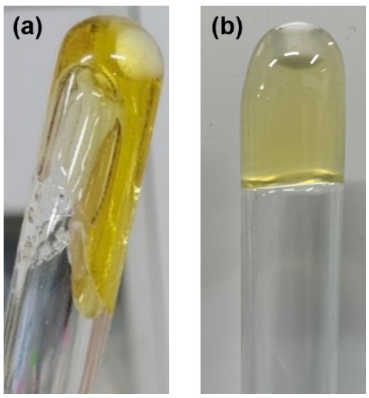

Figure S3. Physical appearance of the PDMA products obtained from the **Fc1**-based photo-Fenton reaction with (**a**) and without (**b**) the trithiocarbonate RAFT agent.

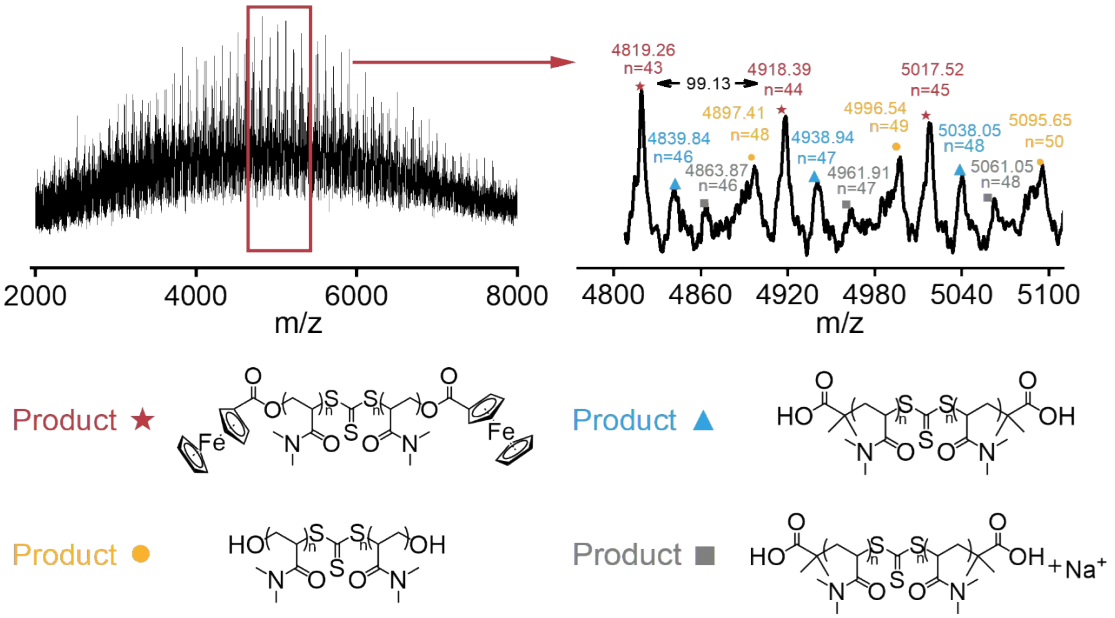

Figure S4. MALDI-TOF full spectrum and magnification of part of the spectrum of $PDMA_{100}$, possible chemical structures corresponding to the mass analysis. [DMA] = 5 M, [**Fc1**] = 1.25 mM, [H_2O_2] = 75 mM, [bis-TTC] = 25 mM, 460-nm light irradiation for 15 min

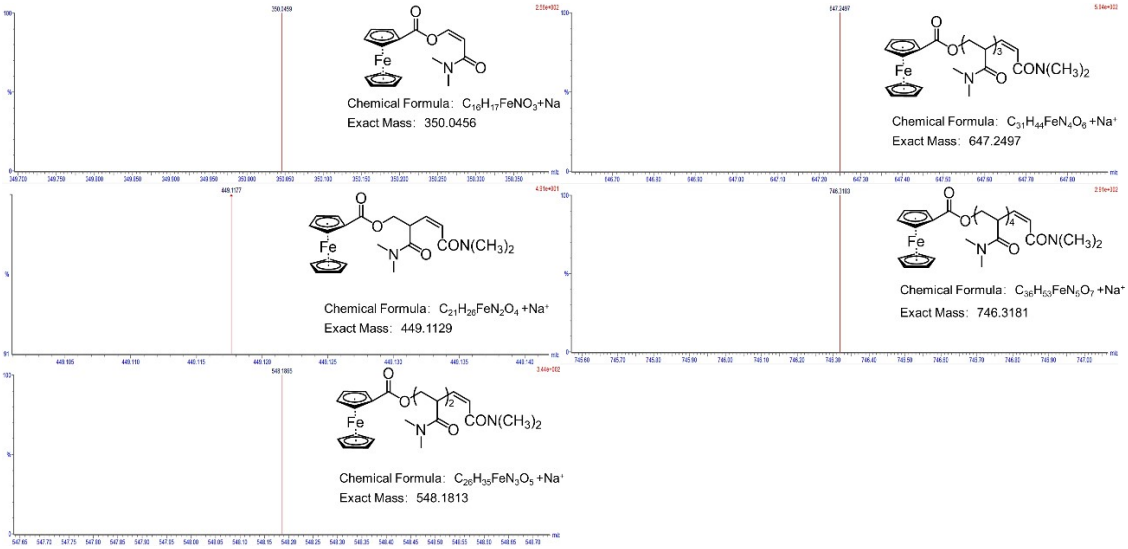

Figure S5. Mass spectra of chemical structures formed through the polymerization of DMA in the absence of a RAFT reagent, subsequent to the reaction of radical FcCOO• with the monomer.

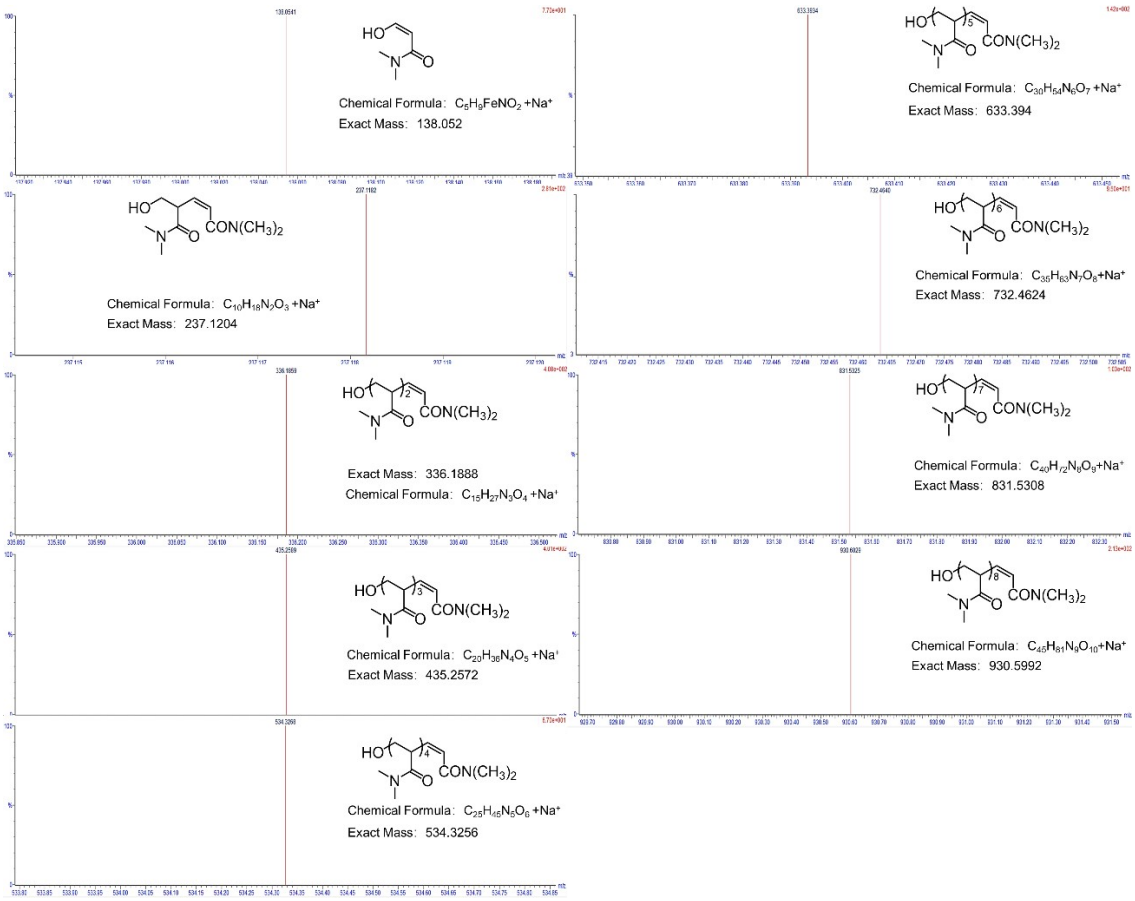

Figure S6. Mass spectra of chemical structures formed through the polymerization of DMA in the absence of a RAFT reagent, subsequent to the reaction of radical •OH with the monomer.

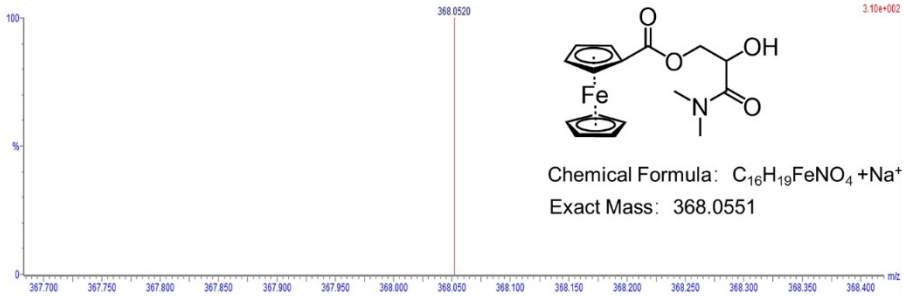

Figure S7. Mass spectrum of the chemical structure formed through the polymerization of DMA in the absence of a RAFT reagent, subsequent to the reaction of the dual radicals of FcCOO• and •OH with the monomer.

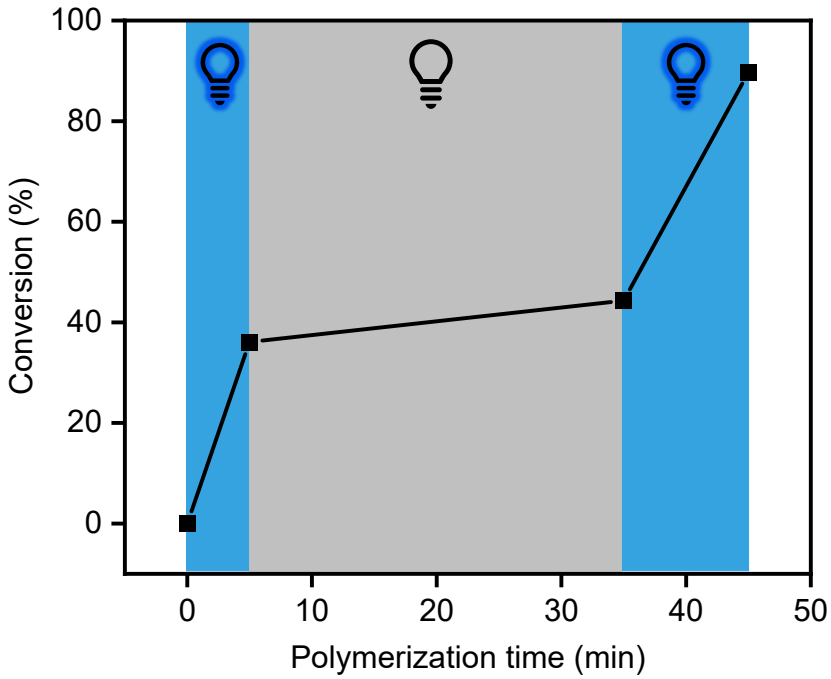

Figure S8. Temporal control of polymerization through the measurement of monomer conversion over time with intermittent light exposure.

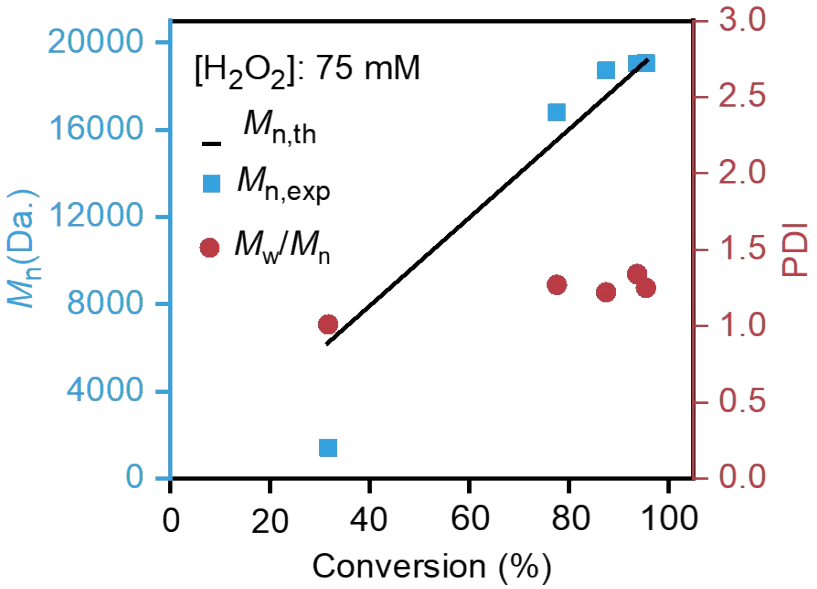

Figure S9. Molecular weight and polydispersity index evolution with monomer conversion at a H_2O_2 concentration of 75 mM.

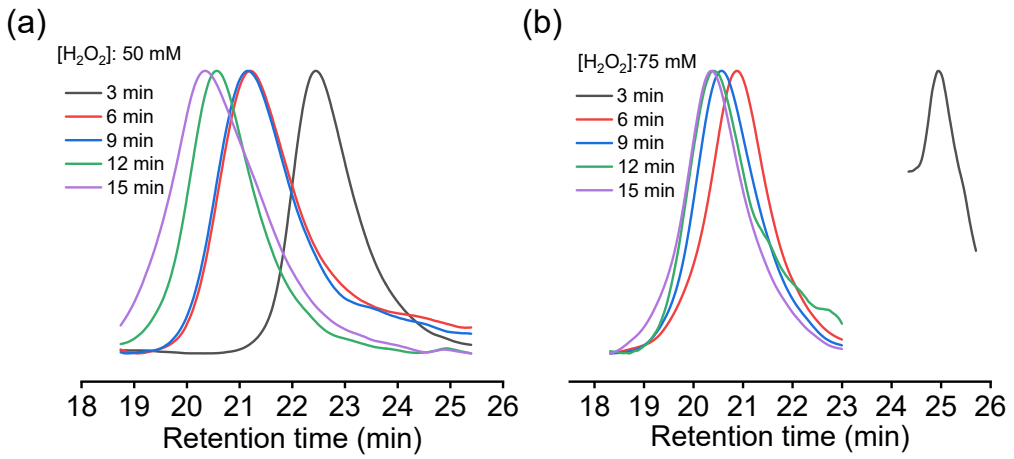

Figure S10. GPC curves depicting the polymerization kinetics at hydrogen peroxide concentrations of 50 mM (a) and 75 mM (b), respectively.

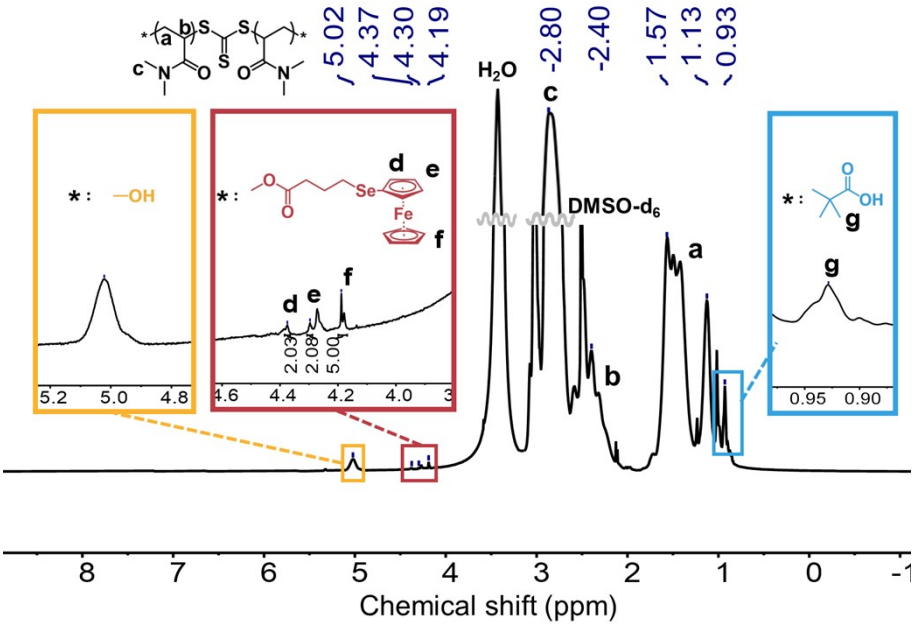

Figure S11. ^{1}H NMR spectra of **Fc2**-PDMA-**Fc2** obatined after 72 hours of dialysis.

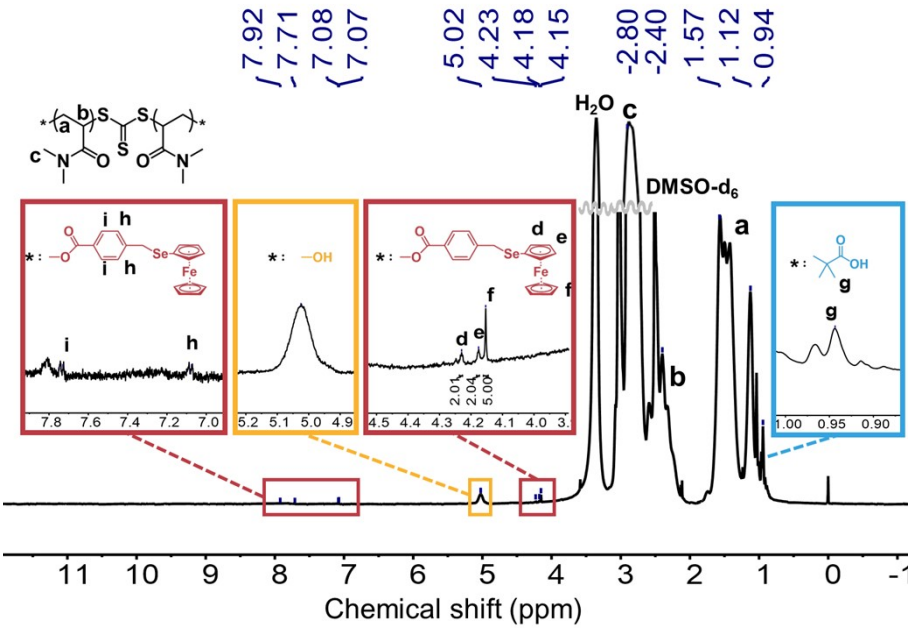

Figure S12. ^{1}H NMR spectra of **Fc3**-PDMA-**Fc3** obained after 72 hours of dialysis.

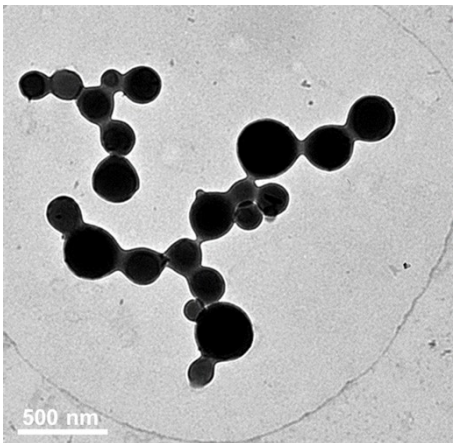

Figure S13. TEM image of the self-assembled structures formed by **Fc2**-PDMA$_{25}$-**Fc2** synthesized with a **Fc2**:[bis-TTC] ratio of 0.05:1.

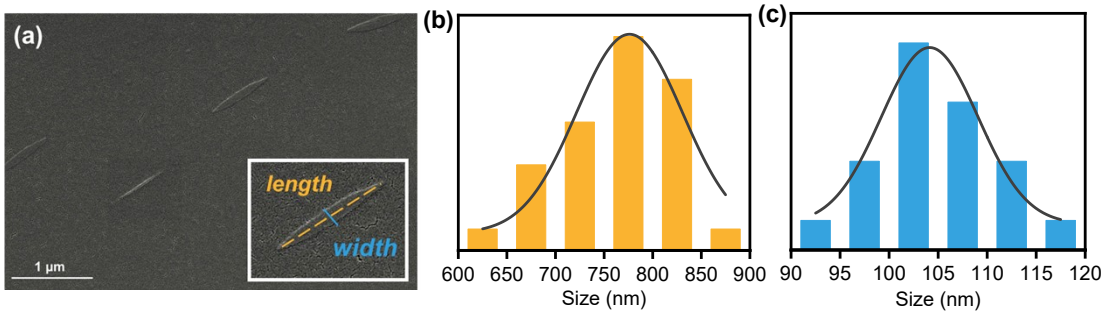

Figure S14. SEM image (**a**), size (length) distribution (**b**) and size (width) distribution (**c**) curve of the self-assembled structures formed by **Fc2**-PDMA$_{50}$-**Fc2** synthesized

with a **Fc2**:[bis-TTC] ratio of 0.05:1.

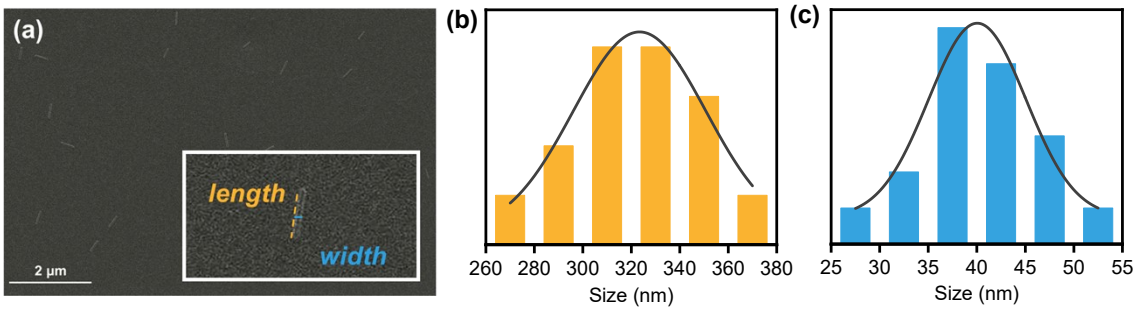

Figure S15. SEM image (**a**), size (length) distribution (**b**) and size (width) distribution (**c**) curve of the self-assembled structures formed by **Fc2**-PDMA$_{100}$-**Fc2** synthesized with a **Fc2**:[bis-TTC] ratio of 0.05:1.

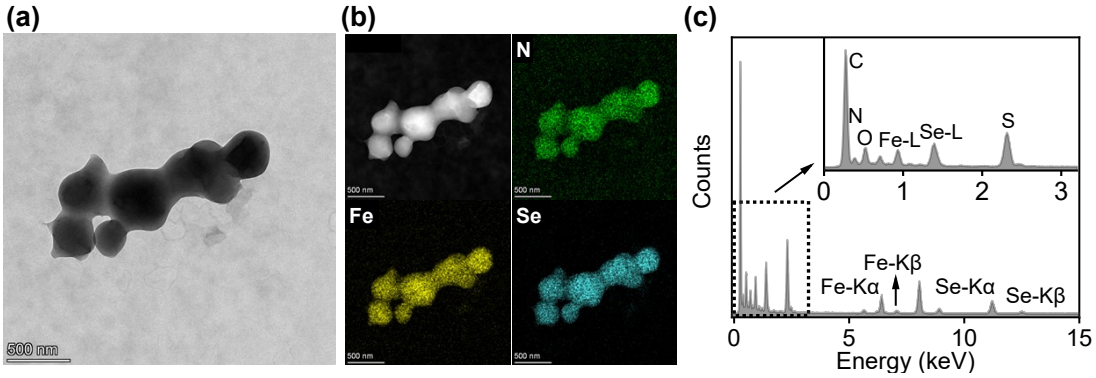

Figure S16. TEM image (**a**), energy dispersive X-ray mapping images (**b**), and EDS spectrum (**c**) of the self-assembled structures formed by **Fc3**-PDMA$_{25}$-**Fc3** synthesized with a **Fc3**:[bis-TTC] ratio of 0.05:1. The inset in panel (**c**) provided a magnified spectrum of panel (**b**) within the energy range of 0 to 3 KeV.

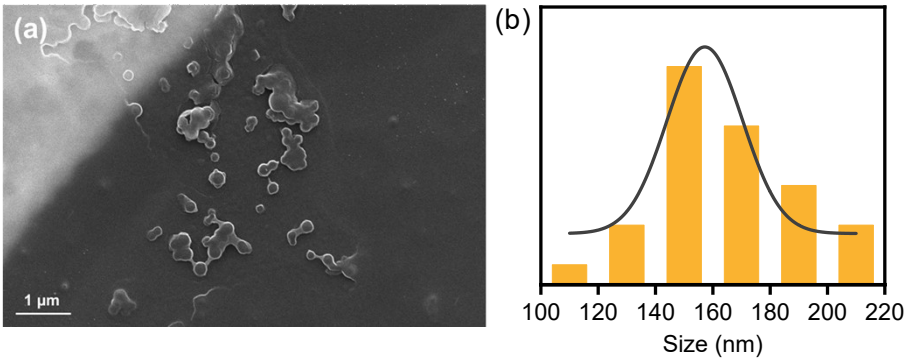

Figure S17. SEM image (**a**) and size distribution curve (**b**) of the self-assembled structures formed by **Fc3**-PDMA$_{25}$-**Fc3** synthesized with a **Fc3**:[bis-TTC] ratio of 0.05:1.

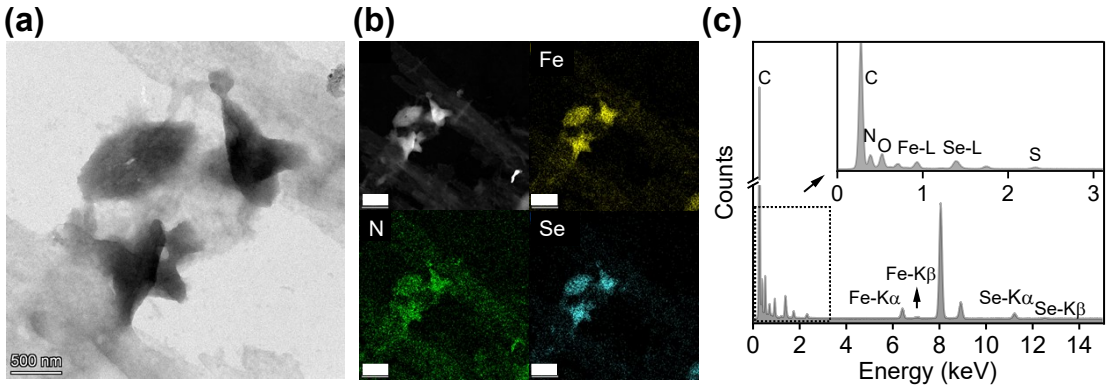

Figure S18. TEM image (**a**), energy dispersive X-ray mapping images (**b**), and EDS spectrum (**c**) of the self-assembled structures formed by **Fc3**-PDMA$_{50}$-**Fc3** synthesized with a **Fc3**:[bis-TTC] ratio of 0.05:1. Scale bar for panel (**b**), 1 μm. The inset in panel (**c**) provided a magnified spectrum of panel (**b**) within the energy range of 0 to 3 KeV.

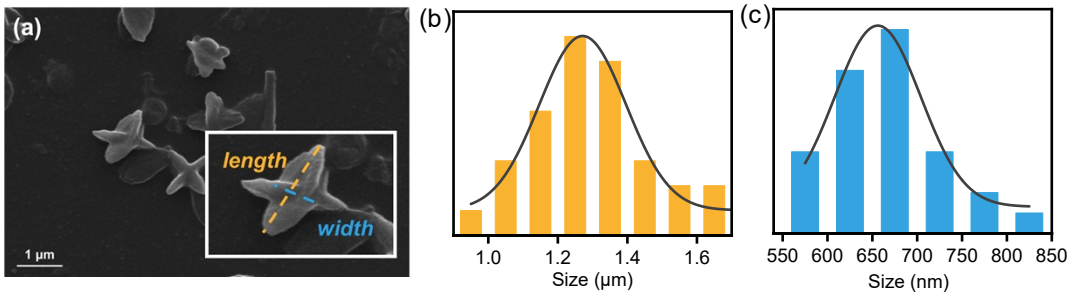

Figure S19. SEM image (**a**), size (length) distribution (**b**) and size (width) distribution (**c**) curve of the self-assembled structures formed by **Fc3**-PDMA$_{50}$-**Fc3** synthesized with a **Fc3**:[bis-TTC] ratio of 0.05:1.

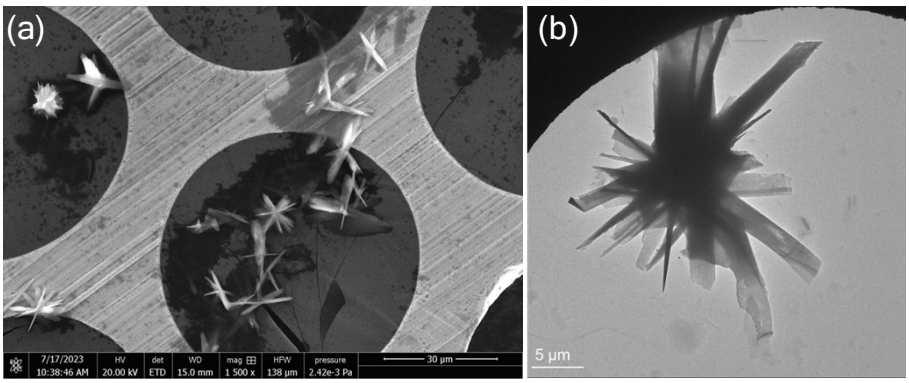

Figure S20. SEM (**a**) and TEM (**b**) image of the self-assembled structures formed by **Fc3**-PDMA$_{100}$-**Fc3** synthesized with a **Fc3**:[bis-TTC] ratio of 0.05:1.

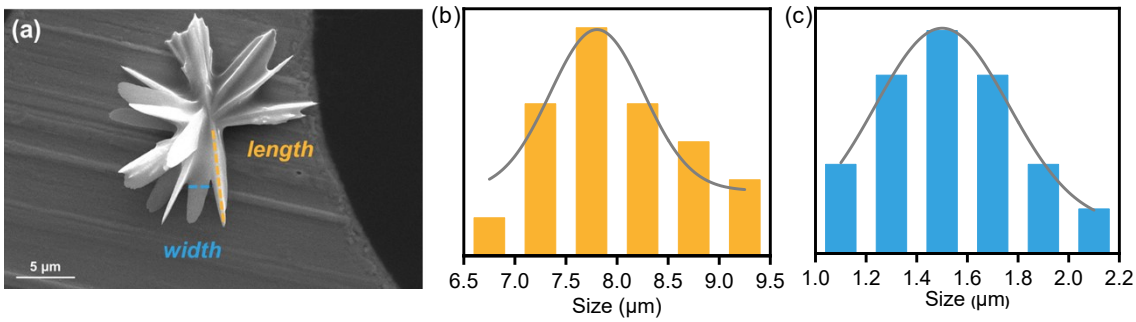

Figure S21. SEM image (**a**), size (length) distribution (**b**) and size (width) distribution (**c**) curve of the self-assembled structures formed by **Fc3**-PDMA$_{100}$-**Fc3** synthesized with a **Fc3**:[bis-TTC] ratio of 0.05:1.

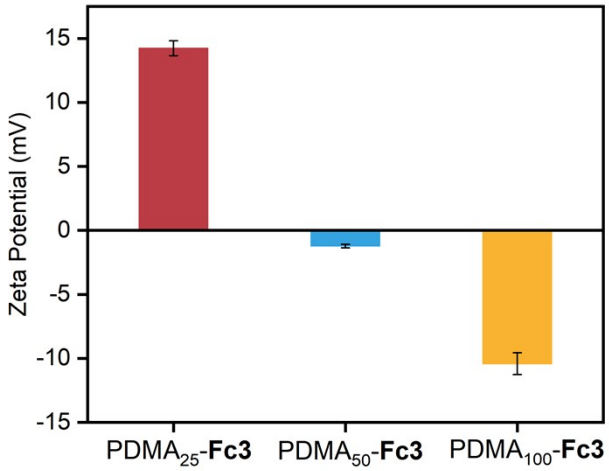

Figure S22. Zeta potential distribution of the self-assembled structures formed by **Fc3**-PDMA-**Fc3** with varying degrees of polymerization, synthesized with a **Fc3**:[bis-TTC] ratio of 0.05:1.

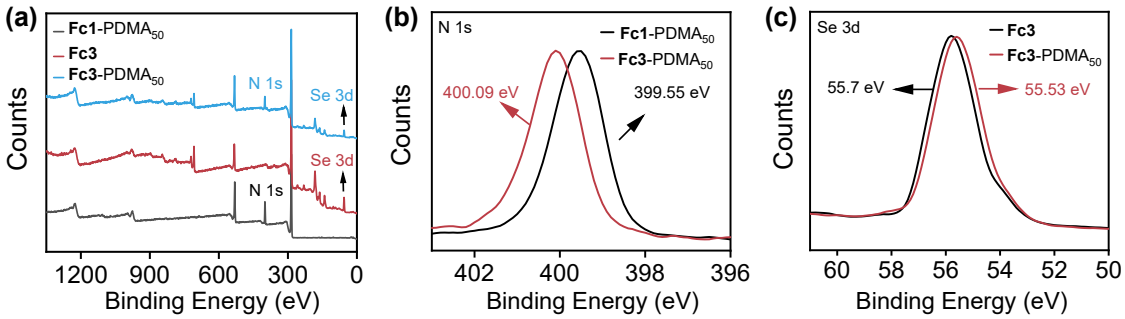

Figure S23. XPS analysis of **Fc1**-PDMA$_{50}$, **Fc3** and **Fc3**-PDMA$_{50}$.

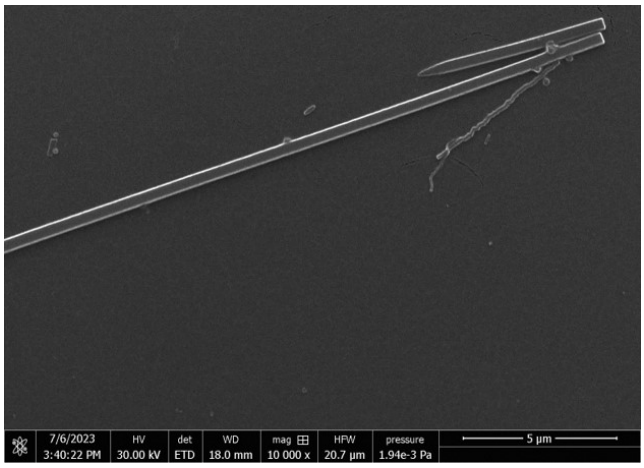

Figure S24. SEM image of the self-assembled structures formed by **Fc3**-$PDMA_{100}$-**Fc3**, synthesized with a **Fc3**:[bis-TTC] ratio of 0.2:1.

Table S1. List of some crystal plane angles (°) within the single-crystal structure of **Fc3.**

Crystal plane angle (°)	$\bar{2}08$	$20\bar{8}$	$12\bar{3}$	$\bar{1}23$
$70\bar{5}$	128.0	51.0	73.0	106.0
$\bar{7}05$	51.0	128.0	106.0	73.0
$32\bar{1}0$	144.0	35.8	31.3	77.6
$\bar{3}210$	35.8	144.0	77.6	31.3
$\bar{5}\bar{2}7$	46.8	133.0	145.6	104.0
$5\bar{2}\bar{7}$	133.0	46.8	104.0	145.6
$\bar{5}27$	75.0	133.1	75.8	34.3
$52\bar{7}$	133.0	46.8	34.3	75.8
$60\bar{9}$	149.0	30.5	68.6	111.3
609	71.0	108.0	94.0	85.7

References

1 J. Zhou, X. Zhu, Q. Cheng, Y. Wang, R. Wang, X. Cheng, J. Xu, K. Liu, L. Li, X. Li, M. Hu, J. Wang, H. Xu, S. Jing and L. Huang, Ferrocene functionalized upconversion nanoparticle nanosystem with efficient Near-Infrared-light-promoted Fenton-like reaction for tumor growth suppression. *Inorg. Chem.*, 2020, **59,** 9177–9187.

2 T. Zhou, Q. Cheng, L. Zhang, D. Zhang, L. Li, T. Jiang, L. Huang, H. Xu, M. Hu

and S. Jing, Ferrocene-functionalized core–shell lanthanide-doped upconversion nanoparticles: NIR light promoted chemodynamic therapy and luminescence imaging of solid tumors. *Chem. Eng. J.*, 2022, **438,** 135637.